



CARDIOVASCULAR, PULMONARY, AND RENAL PATHOLOGY

Diuretics Prevent Thiazolidinedione-Induced Cardiac Hypertrophy without Compromising Insulin-Sensitizing Effects in Mice

Cherng-Shyang Chang,^{*†} Pei-Jane Tsai,^{‡§} Junne-Ming Sung,[¶] Ju-Yi Chen,^{||**} Li-Chun Ho,^{**††} Kumar Pandya,^{‡‡} Nobuyo Maeda,^{‡‡} and Yau-Sheng Tsai^{*†**}

From the Institutes of Basic Medical Sciences* and Clinical Medicine,** the Cardiovascular Research Center,[†] the Department of Medical Laboratory Science and Biotechnology,[‡] and the Research Center of Infectious Disease and Signaling,[§] National Cheng Kung University, Tainan, Taiwan; the Divisions of Nephrology[¶] and Cardiology,^{||} National Cheng Kung University Hospital, Tainan, Taiwan; the Division of Nephrology,^{††} Department of Internal Medicine, E-DA Hospital/I-Shou University, Kaohsiung, Taiwan; and the Department of Pathology and Laboratory Medicine,^{‡‡} University of North Carolina at Chapel Hill, North Carolina

Accepted for publication
October 17, 2013.

Address correspondence to
Yau-Sheng Tsai, Ph.D., 1 Uni-
versity Rd., National Cheng
Kung University, Tainan 701,
Taiwan, ROC. E-mail:
yau-tsai@mail.ncku.edu.tw.

Much concern has arisen regarding critical adverse effects of thiazolidinediones (TZDs), including rosiglitazone and pioglitazone, on cardiac tissue. Although TZD-induced cardiac hypertrophy (CH) has been attributed to an increase in plasma volume or a change in cardiac nutrient preference, causative roles have not been established. To test the hypothesis that volume expansion directly mediates rosiglitazone-induced CH, mice were fed a high-fat diet with rosiglitazone, and cardiac and metabolic consequences were examined. Rosiglitazone treatment induced volume expansion and CH in wild-type and PPAR γ heterozygous knockout (*Pparg*^{+/-}) mice, but not in mice defective for ligand binding (*Pparg*^{P465L/+}). Cotreatment with the diuretic furosemide in wild-type mice attenuated rosiglitazone-induced CH, hypertrophic gene reprogramming, cardiomyocyte apoptosis, hypertrophy-related signal activation, and left ventricular dysfunction. Similar changes were observed in mice treated with pioglitazone. The diuretics spironolactone and trichlormethiazide, but not amiloride, attenuated rosiglitazone effects on volume expansion and CH. Interestingly, expression of glucose and lipid metabolism genes in the heart was altered by rosiglitazone, but these changes were not attenuated by furosemide cotreatment. Importantly, rosiglitazone-mediated whole-body metabolic improvements were not affected by furosemide cotreatment. We conclude that releasing plasma volume reduces adverse effects of TZD-induced volume expansion and cardiac events without compromising TZD actions in metabolic switch in the heart and whole-body insulin sensitivity. (*Am J Pathol* 2014, 184: 442–453; <http://dx.doi.org/10.1016/j.ajpath.2013.10.020>)

Thiazolidinediones (TZDs), including rosiglitazone and pioglitazone, are PPAR γ agonists successfully used for treatment of diabetes mellitus. However, concerns about cardiac adverse effects and congestive heart failure due to TZD treatment have increased in recent years. From a large meta-analysis, Nissen and Wolski¹ reported that rosiglitazone treatment was associated with increased risks of myocardial infarction and cardiovascular death; however, subsequent reports provided a mixed variety of evidence for adverse cardiovascular effects of rosiglitazone and pioglitazone.^{2,3} Controversy over TZDs has undermined confidence in drugs targeting PPAR γ , and a better understanding of adverse

effects is needed to develop safe antidiabetic therapies targeting PPAR γ .

PPAR γ activation is known to induce genes involved in lipid uptake and storage, glucose utilization, and energy expenditure in adipose tissue. Moreover, PPAR γ activation exhibits a variety of systemic effects and, most remarkably, it directs a greater portion of lipid to adipose tissue.⁴ In

Supported by grants from the Taiwan National Science Council (NSC-98-2320-B-006-009 and NSC-100-2321-B-006-016 to Y.S.T.), Taiwan National Health Research Institutes (NHRI-EX102-10231SI to Y.S.T.), and National Cheng Kung University (NCKU) Aim for the Top University Project and from the NIH (R01-HL042630 to N.M.).

addition to adipose tissue, other tissues, including heart and kidney, express PPAR γ at relatively low levels.⁴ Cardiac hypertrophy (CH) is accompanied by fetal gene reprogramming, including re-expression of natriuretic peptides and switches in contractile proteins and metabolic enzymes.⁵ Decreases in fatty acid oxidation and increases in glucose utilization lead to a change in preference of nutrient usage from fatty acids to carbohydrates in the heart. Interference with fatty acid or glucose utilization in rodents has been shown to induce CH or heart failure, suggesting that alteration in energy substrate is sufficient for induction of CH.^{5,6} Furthermore, rosiglitazone-treated mice show attenuated activation of genes involved in fatty acid oxidation and lipid uptake in the heart.⁷ Because gene products downstream of PPAR γ are critical in regulation of glucose and lipid metabolism in the heart, it is reasonable to speculate that PPAR γ activation induces CH through modulation of nutrient metabolism.

TZDs may induce CH either directly, acting on the heart, or indirectly, through effects on noncardiac tissues. For example, it has been established that rosiglitazone stimulates sodium reabsorption by increasing renal tubule transporters, including *Atp1a1*, *NHE3*, and *Npt2* in the proximal convoluted tubule, and *Nkcc2* in the thick ascending limb.⁸ Moreover, renal PPAR γ activation has been shown to up-regulate *ENaC γ* , a subunit of sodium transporter in the collecting duct.^{9,10} Up-regulation of these renal sodium transporters increases sodium reabsorption and further induces volume expansion. Chronic volume overload is initially compensated for by CH, but eventually leads to cardiomyopathy and heart failure if the condition is not resolved.¹¹ However, although TZD-induced CH has been associated with increases in plasma volume and changes in nutrient preferences, causative roles have not yet been established. There has been no direct evidence showing that a release of plasma volume or blocking of sodium reabsorption ameliorates TZD-induced CH. Moreover, efficacy of diuretics in alleviating PPAR γ agonist-induced hemodilution in humans remains debatable.^{12,13}

We hypothesized that TZD-induced CH is directly mediated through volume expansion. To test this hypothesis, we released TZD-induced volume overload by feeding mice diuretics [furosemide, amiloride, spironolactone, or trichlormethiazide (TCM)] and then examined PPAR γ dependence by using PPAR γ heterozygous knockout (*Pparg*^{+/-}) mice and a mutant strain (*Pparg*^{P465L/+}) that is defective in the ligand-binding competence of PPAR γ .¹⁴ Our findings indicate that simultaneous treatment with furosemide inhibits CH without affecting TZD-induced metabolic changes in the heart or compromising whole-body insulin-sensitizing effects of TZD.

Materials and Methods

Mice

The *Pparg*^{P465L/+} mutation¹⁴ was transferred onto a C57BL/6 genetic background by backcrossing more than 12

generations, and *Pparg*^{P465L/+} and their wild-type (WT) littermates were used for experiments. *Pparg*^{+/-} mice, provided by Dr. Ronald Evans, were maintained on a 129S6 background and were mated with WT C57BL/6 mice, obtained from the National Laboratory Animal Center (Taipei, Taiwan), to generate F1 littermates. Male mice at 8 weeks of age were fed a high-fat diet (58% fat energy) (58R2; Test-Diet, St. Louis, MO) or a high-fat diet blended with 10 mg/kg per day rosiglitazone or 40 mg/kg per day pioglitazone for 4 weeks. In diuretic treatment groups, rosiglitazone-treated mice were simultaneously treated with diuretics for 4 weeks; 0.1 mg/mL furosemide or 0.02 mg/mL amiloride was added to drinking water, and 30 mg/kg per day spironolactone or 15 mg/kg per day TCM was blended with a high-fat diet supplemented with rosiglitazone. For a furosemide withdrawal experiment, furosemide administration was discontinued after 4 weeks of cotreatment, and rosiglitazone treatment was continued for a further 1 or 2 weeks. Protocols were approved by the Institutional Animal Care and Use Committees of National Cheng Kung University.

Plasma Volume Analysis

After anesthesia, 0.1 mL of 1 mg/mL Evans Blue dye solution was injected through the portal vein, and after 3 minutes blood was collected from the vena cava. Plasma volume was calculated as the total amount of injected dye divided by the concentration of dye in plasma as measured by spectrophotometer at 620 nm.

Sodium Analysis

For 24-hour urine collection, mice were housed in single-mouse metabolic cages (Tecniplast, Buguggiate, Italy). Urinary sodium concentrations were measured on day 5 of treatment using a Dri-Chem 4000i chemistry analyzer (Fujifilm, Tokyo, Japan). Daily sodium excretion was calculated as sodium concentration multiplied by urine volume and then divided by body weight.

Histological Analysis of Heart

Anesthetized mice were perfused with 10% buffered formalin. A midventricular slice of myocardium was embedded in paraffin. Sections were cut, stained with H&E, and analyzed using ImageJ software version 1.42q (NIH, Bethesda, MD). For examining apoptosis, paraffin sections of heart were analyzed by TUNEL assay (Clontech Laboratories, Mountain View, CA). For immunohistochemical staining, sections were deparaffinized, blocked, and incubated overnight with primary antibodies against p-Erk1/2 (Cell Signaling Technology, Danvers, MA). Secondary antibody staining was performed using a kit (Vector Laboratories, Burlingame, CA), and detection was performed using a 3,3'-diaminobenzidine substrate chromogen solution (Dako, Carpinteria, CA).

RNA Analysis

Tissues were stored in Ambion RNAlater stabilization solution (Life Technologies, Carlsbad, CA), and total RNA was extracted with REzol isolation reagent (Protech Technology Enterprise, Taipei, Taiwan). Samples of mRNA were analyzed with SYBR Green–based real-time quantitative reverse transcription PCR (RT-qPCR), with *Gapdh* as the reference gene in each reaction.

Echocardiography

Isoflurane-anesthetized mice were placed on a heating pad in a supine position. Echocardiographic images were obtained using a Vevo 770 microimaging system with a 25-MHz probe (VisualSonics, Toronto, ON, Canada). Parasternal short-axis views of left ventricle (LV) were acquired at the papillary muscle level, and M-mode records were obtained.

Western Blotting

Total protein (20 μ g) from the lower portion of hearts was separated by SDS-PAGE, transferred to polyvinylidene difluoride membranes (Pall Gelman Laboratory, Ann Arbor, MI), and probed with antibodies. Immunoreactive proteins were detected using an enhanced chemiluminescence Western blotting detection system (GE Healthcare, Little Chalfont, UK).

Statistical Analysis

Statistical analyses were performed using Student's *t*-test or one-way analysis of variance followed by Fisher's least significant difference (LSD) multiple comparison test. Differences were considered statistically significant at $P < 0.05$. Data are expressed as means \pm SEM.

Results

Rosiglitazone Induces Volume Expansion and CH through PPAR γ

To induce insulin resistance, all experimental mice were fed a high-fat diet for 4 weeks with or without rosiglitazone. The rosiglitazone-supplemented diet induced hemodilution, reflected by decreased hematocrit, and an increase in heart weight (HW) in WT mice in a dose-dependent manner (Supplemental Figure S1). Because treatment with rosiglitazone at 10 mg/kg per day for 4 weeks induced a significant increase in the heart weight/body weight ratio (HW/BW), compared with those on a control diet without rosiglitazone supplement, we chose this dosage for experiments. The same rosiglitazone-supplemented regular chow also induced hemodilution and CH in WT mice (data not shown).

To investigate whether the effects of rosiglitazone on hemodilution and CH are dependent on PPAR γ , *Pparg*^{+/-} and *Pparg*^{P465L/+} mice were used. Basic cardiac phenotypes of *Pparg*^{+/-} and *Pparg*^{P465L/+} mice appear normal.^{14–16} Hematocrit and HW of *Pparg*^{+/-} mice on the control diet did not differ from those of WT mice. Furthermore, rosiglitazone treatment decreased hematocrit and increased HW in both WT and *Pparg*^{+/-} mice, and to similar extent (Figure 1, A–C). These findings indicate that rosiglitazone can nevertheless cause volume expansion and CH, despite a 50% reduction in PPAR γ expression.

The P465L mutation in the ligand-binding domain of PPAR γ suppresses PPAR γ activation in a dominant-negative fashion.¹⁴ Nevertheless, basal hematocrit and HW of the heterozygous *Pparg*^{P465L/+} mice did not differ from those of WT mice. Interestingly, however, the effect of rosiglitazone on hemodilution was blunted in *Pparg*^{P465L/+} mice (Figure 1A). Consistent with the absence of volume expansion, rosiglitazone treatment did not induce an increase in HW in *Pparg*^{P465L/+} mice (Figure 1, B and C).

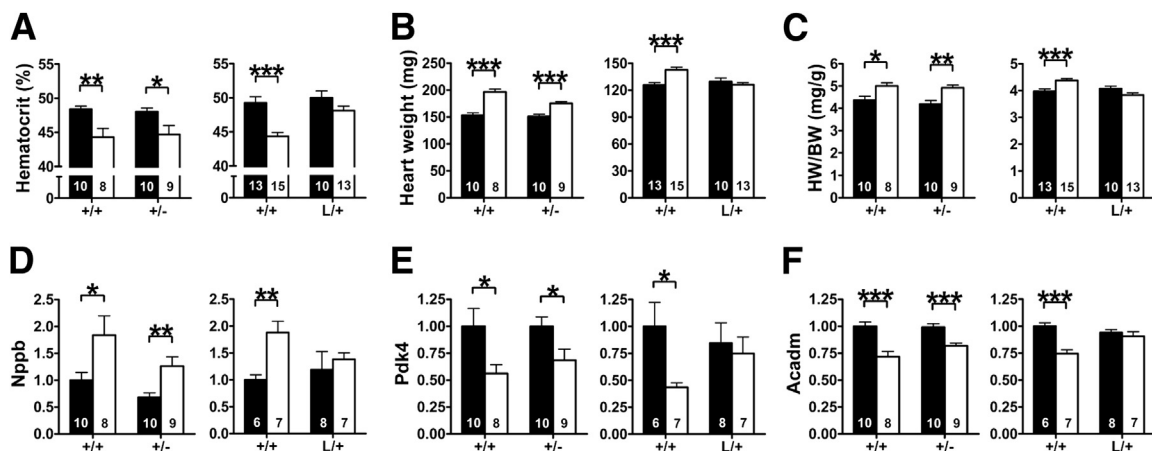


Figure 1 Volume expansion and CH in the hearts of rosiglitazone-treated mice of three genotypes: *Pparg*^{+/+} (WT), *Pparg*^{+/-} (heterozygous knockout), and *Pparg*^{P465L/+} (defective for ligand binding). **A–C:** Hematocrit (**A**), HW (**B**), and HW/BW ratio (**C**). **D–F:** mRNA levels of hypertrophic (**D**) and metabolism (**E** and **F**) genes, relative to average expression in *Pparg*^{+/+} mice without rosiglitazone treatment. Data are expressed as means \pm SEM. $n = 6$ to 15 mice per group (indicated on data bars). * $P < 0.05$, ** $P < 0.01$, and *** $P < 0.001$, Student's *t*-test. Con, control (black bars); Rosi, rosiglitazone (white bars).

No differences were found in basal expression of natriuretic peptide or in glucose and lipid metabolism among WT, *Pparg*^{+/-}, and *Pparg*^{P465L/+} mice. However, although both WT and *Pparg*^{+/-} mice responded to rosiglitazone similarly, with altered expression of genes for natriuretic peptide [natriuretic peptide type B (*Nppb*)] and metabolism [pyruvate dehydrogenase kinase isoenzyme 4 (*Pdk4*) and acyl-coenzyme A dehydrogenase, medium chain (*Acadm*)], expression of these genes was not affected in rosiglitazone-treated *Pparg*^{P465L/+} mice (Figure 1, D–F).

Taken together, these findings demonstrate that rosiglitazone-induced volume expansion and CH, as well as dysregulation in hypertrophic and metabolism genes, all require intact ligand-binding ability of PPAR γ . In contrast, a 50% normal level of PPAR γ expression is sufficient to mediate dysregulation of both hypertrophic and metabolism gene expression in the heart.

Cotreatment with Furosemide Prevents Rosiglitazone-Induced Volume Expansion and CH

To determine whether volume expansion is causative of rosiglitazone-induced HW gain, we next fed WT mice a diet

supplemented with both rosiglitazone and furosemide, to release volume expansion. Treatment with rosiglitazone for 5 days significantly lowered urinary sodium excretion, which is inhibited by furosemide cotreatment (Figure 2A). After 4 weeks of cotreatment, furosemide prevented increases in plasma volume and HW (Figure 2, B–E). These findings directly indicate that releasing volume expansion is protective against increases in HW caused by rosiglitazone treatment. Furthermore, we found a strong inverse correlation between HW/BW ratio and hematocrit ($r = -0.4205$; $P < 0.0001$) (Figure 2F). This observation further supports causality between volume expansion and HW gain. Finally, we investigated the durability of furosemide effect and found that volume expansion and CH reappeared after discontinuing furosemide administration for 1 week (Figure 2, G and H, and Supplemental Figure S2).

No notable change in ventricular fibrosis was found in rosiglitazone-treated hearts (data not shown). Gross examination showed that both long and short axes of the heart were increased by rosiglitazone treatment, and that these increases were blunted by cotreatment with furosemide (Figure 2I and Supplemental Figure S3). Morphometric analyses of the dissected heart did not reveal any differences in LV wall thickness among the three groups; however, LV

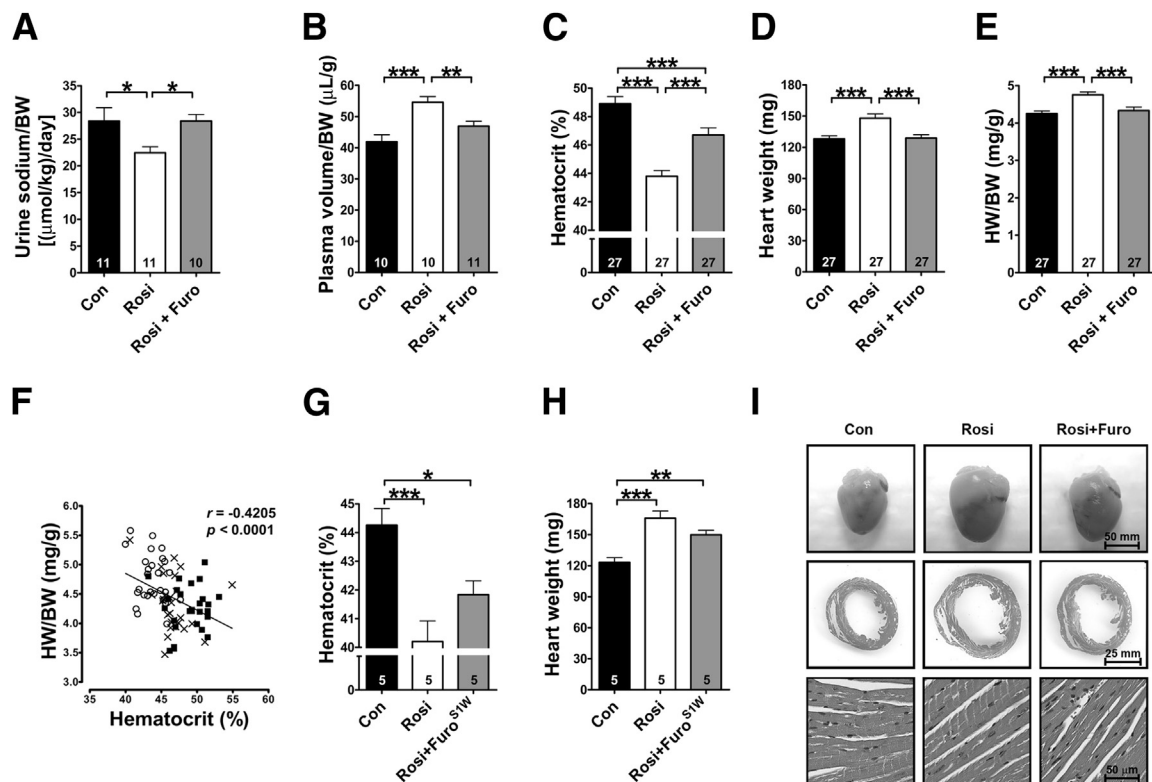


Figure 2 Effects of furosemide on rosiglitazone-induced volume expansion and CH. **A–E:** Daily sodium excretion expressed as the ratio of urinary sodium to BW (**A**), the ratio of plasma volume to BW (**B**), hematocrit (**C**), HW (**D**), and HW/BW ratio (**E**) of control, rosiglitazone-treated, and rosiglitazone+furosemide-treated mice. **F:** Correlation between HW/BW ratio and hematocrit in control (squares), rosiglitazone-treated (circles), and rosiglitazone+furosemide-treated mice (crosses). $n = 27$ mice per group. **G** and **H:** Hematocrit (**G**) and HW (**H**) in the furosemide withdrawal experiment. Mice were continually treated with rosiglitazone for 1 week after discontinuing furosemide cotreatment (S1W). **I:** Gross appearance (**top row**), cross section (**middle row**), and tissue section (**bottom row**) of mouse hearts. Data are expressed as means \pm SEM. $n = 5, 10, 11,$ or 27 mice per group, as indicated on data bars (**A–E, G, H**). * $P < 0.05$, ** $P < 0.01$, and *** $P < 0.001$, Fisher's LSD test. Furo, furosemide.

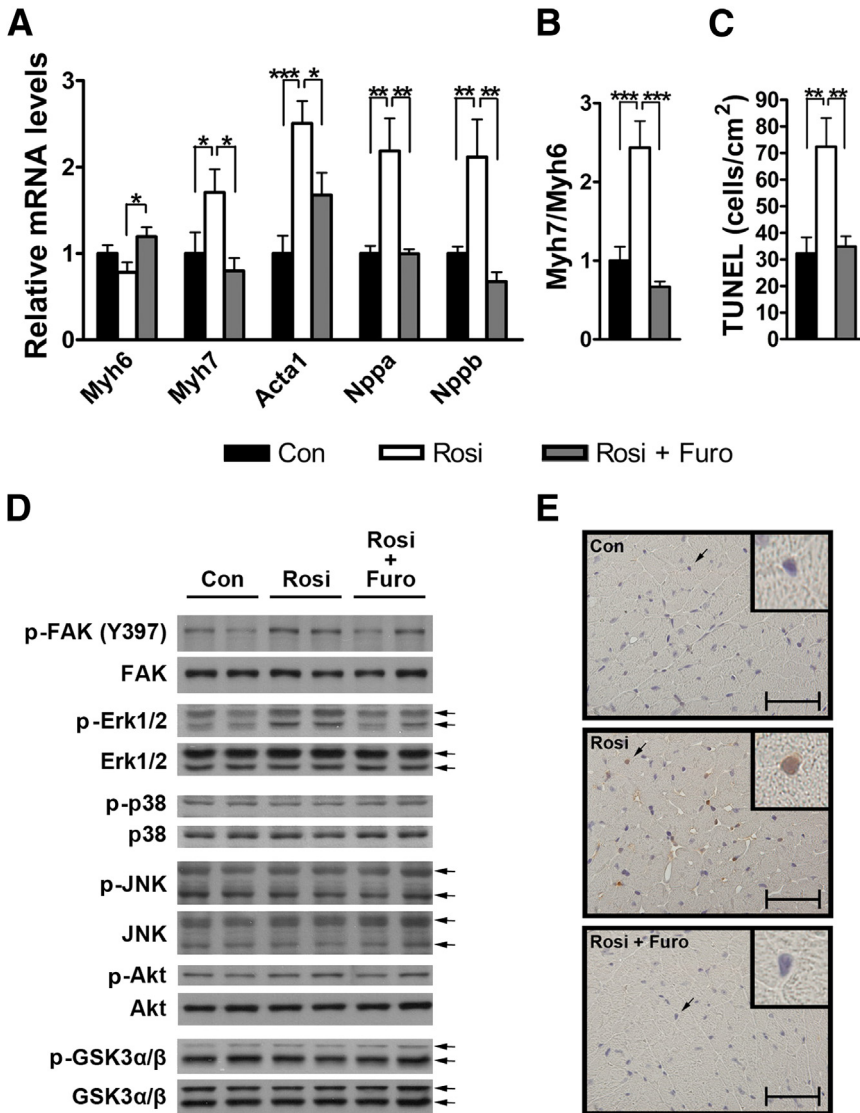


Figure 3 Gene expression and signaling pathways in rosiglitazone-induced CH. **A–C**: Expression of contractile and natriuretic peptide genes (**A**), Myh7/Myh6 ratio (**B**), and the number of TUNEL-positive cells (**C**) in whole sections of hearts of control, rosiglitazone-treated, and rosiglitazone+furosemide-treated mice. mRNA levels are expressed relative to average expression in control mice. **D**: Immunoblot analyses of phosphorylation of FAK, Erk1/2, p38, JNK, Akt, and GSK3α/β in the heart. Each band represents tissue extract from a single mouse; **arrows** indicate different molecular weights of the protein isoforms. **E**: Immunohistochemical staining of p-Erk1/2 (brown) in the heart. In each image, a cell marked by an **arrow** is shown at higher magnification in the **inset**. Data are expressed as means ± SEM. *n* = 6 mice per group. **P* < 0.05, ***P* < 0.01, and ****P* < 0.001, Fisher's LSD test. Scale bar = 50 μm.

chamber size appeared larger in the rosiglitazone treatment group, and this was inhibited by furosemide cotreatment. Light microscopic examination revealed no differences in cardiomyocyte diameters or nucleus size among the three groups.

CH and stressed heart are known to be associated with fetal gene reprogramming and cardiomyocyte apoptosis.⁵ Rosiglitazone treatment tended to decrease mRNA levels of myosin heavy polypeptide 6 (*Myh6*) and significantly increased mRNA levels of myosin heavy polypeptide 7 (*Myh7*) (Figure 3A), resulting in a significant increase in Myh7/Myh6 ratio (Figure 3B). Rosiglitazone treatment also significantly increased mRNA levels of skeletal muscle actin α1 (*Acta1*), natriuretic peptide type A (*Nppa*), and *Nppb*. Cotreatment with furosemide did not increase mRNA levels of *Myh7*, *Acta1*, *Nppa*, or *Nppb*, nor did it alter Myh7/Myh6 ratio or decrease mRNA levels of *Myh6*. Furthermore, the number of apoptotic cells, as indicated by

TUNEL staining, was significantly increased in the hearts of rosiglitazone-treated mice but was unchanged in the hearts of rosiglitazone+furosemide-treated mice (Figure 3C).

Next, we evaluated cardiac function by echocardiography (Table 1). Rosiglitazone treatment alone significantly increased systolic and diastolic LV chamber size, whereas furosemide cotreatment attenuated systolic chamber size and tended to decrease diastolic chamber size. No notable changes were found in stroke volume and cardiac output; however, fractional shortening and ejection fraction were significantly decreased by rosiglitazone treatment, and these changes were blunted by furosemide cotreatment. These findings indicate that rosiglitazone-impaired cardiac function can be inhibited by furosemide-mediated release of volume overload. Taken together, the fetal gene reprogramming, apoptosis of cardiomyocytes, and functional changes are consistent with our hypothesis that rosiglitazone treatment causes CH and that this CH is prevented by

Table 1 Echocardiographic Measurements

Measure	Control	Rosiglitazone	Rosiglitazone + furosemide
Sample size	<i>n</i> = 5	<i>n</i> = 5	<i>n</i> = 6
LVDd (mm)	4.14 ± 0.09	4.76 ± 0.14**	4.58 ± 0.11*
LVDs (mm)	2.72 ± 0.08	3.63 ± 0.13***	3.29 ± 0.09**†
LVEVd (mL)	0.076 ± 0.004	0.107 ± 0.007**	0.097 ± 0.006*
LVEVs (mL)	0.028 ± 0.002	0.056 ± 0.005***	0.044 ± 0.003**†
Stroke volume (mL)	0.048 ± 0.002	0.050 ± 0.002	0.053 ± 0.003
Cardiac output (mL/min)	16.9 ± 0.9	17.3 ± 1.0	16.9 ± 1.4
FS (%)	34.36 ± 0.74	23.85 ± 0.62***	28.31 ± 0.83***†
EF (%)	63.71 ± 1.04	47.5 ± 1.12***	54.67 ± 1.26***†

P* < 0.05, *P* < 0.01, and ****P* < 0.001 versus control, Fisher's LSD test.

†*P* < 0.05, ††*P* < 0.001 versus rosiglitazone, Fisher's LSD test.

EF, ejection fraction; FS, fractional shortening; LVDd, left ventricular diastolic diameter; LVDs, left ventricular systolic diameter; LVEVd, left ventricular end-diastolic volume; LVEVs, left ventricular end-systolic volume.

releasing volume expansion, despite continued treatment with rosiglitazone.

Rosiglitazone-Induced CH Is Mediated through Erk1/2 Signaling

Because focal adhesion kinase (FAK) and mitogen-activated protein kinases (MAPKs) are important mediators of CH,^{17,18} we analyzed signaling pathways in relation to volume expansion and CH. Rosiglitazone treatment induced phosphorylation of FAK and Erk1/2, and furosemide cotreatment inhibited these effects (Figure 3D). In contrast, phosphorylation of p38, JNK, Akt, and GSK3α/β was not affected by rosiglitazone or rosiglitazone+furosemide treatment. Immunohistochemical analysis confirmed nuclear localization of p-Erk1/2 in cardiomyocytes of rosiglitazone-treated mice; nuclear localization was absent in cells of mice cotreated with furosemide (Figure 3E). These findings suggest that Erk1/2 is a volume expansion-dependent signal leading to rosiglitazone-induced CH.

Pioglitazone-Induced CH Is Also Mediated through Volume Expansion

Although a retrospective cohort study showed relatively lesser cardiac risk with pioglitazone than with rosiglitazone,¹⁹ induction of CH by pioglitazone has been reported.²⁰ In the present study, feeding mice with a diet containing pioglitazone for 4 weeks reduced hematocrit and increased HW in a dose-dependent fashion (Supplemental Figure S4). Pioglitazone at a dose of 40 mg/kg per day induced cardiac effects similar to those induced by rosiglitazone at 10 mg/kg per day. Cotreatment with furosemide protected mice from pioglitazone-mediated decrease in hematocrit and increase in heart mass (Figure 4, A–C), and there was an inverse correlation between HW/BW ratio and hematocrit (*r* = −0.5170; *P* = 0.0012) (Figure 4D). Consistently, pioglitazone treatment induced reprogramming of hypertrophic genes and increased phosphorylation of FAK and Erk1/2, and cotreatment with

furosemide ameliorated these changes (Figure 4, E–G). These findings indicate that, as for rosiglitazone, volume expansion is an important factor causing CH in response to pioglitazone treatment. Overall effects of pioglitazone and rosiglitazone on the heart are summarized in Supplemental Table S1.

Spirolactone and TCM Prevent Rosiglitazone-Induced Volume Expansion and CH

Rosiglitazone treatment significantly increased mRNA levels of ENaCα, ENaCβ, and ENaCγ (*Scnn1a*, *Scnn1b*, and *Scnn1g*, respectively), and protein levels of ENaCγ in the kidney (Figure 5, A and B). In addition, rosiglitazone treatment significantly increased mRNA levels of Npt2 (*Slc34a1*), Atp1a1, and Nkcc2 (*Slc12a1*), but not NHE3 (*Slc9a3*) or NCC (*Slc12a3*). These findings suggest that renal transporters other than ENaC may be involved in rosiglitazone-induced water reabsorption; this could explain the effective protection by furosemide, which blocks Nkcc2.

Next, we tested the effects of other diuretic agents. Cotreatment with amiloride, a specific ENaC blocker, did not significantly attenuate the decrease of urinary sodium excretion (Supplemental Figure S5). Consequently, rosiglitazone-induced plasma volume expansion and CH were not inhibited by amiloride. In contrast, cotreatment with either spironolactone (an aldosterone receptor blocker which indirectly inactivates ENaC) or TCM (a specific NCC blocker) inhibited the rosiglitazone-induced decrease of urinary sodium excretion and modulated rosiglitazone effects on plasma volume expansion and CH (Figure 5, C–F).

Glucose and Lipid Metabolism Genes Are Not Dependent on Volume Expansion in TZD-Induced CH

Because PPARγ is important in regulation of nutrient utilization, we next investigated whether genes related to glucose and lipid metabolism are involved in rosiglitazone-mediated CH. mRNA levels of glucose transporter Glut1 (*Slc2a1*) and Glut4 (*Slc2a4*), glycolysis (hexokinase 2; *Hk2*), and glycogenosis and

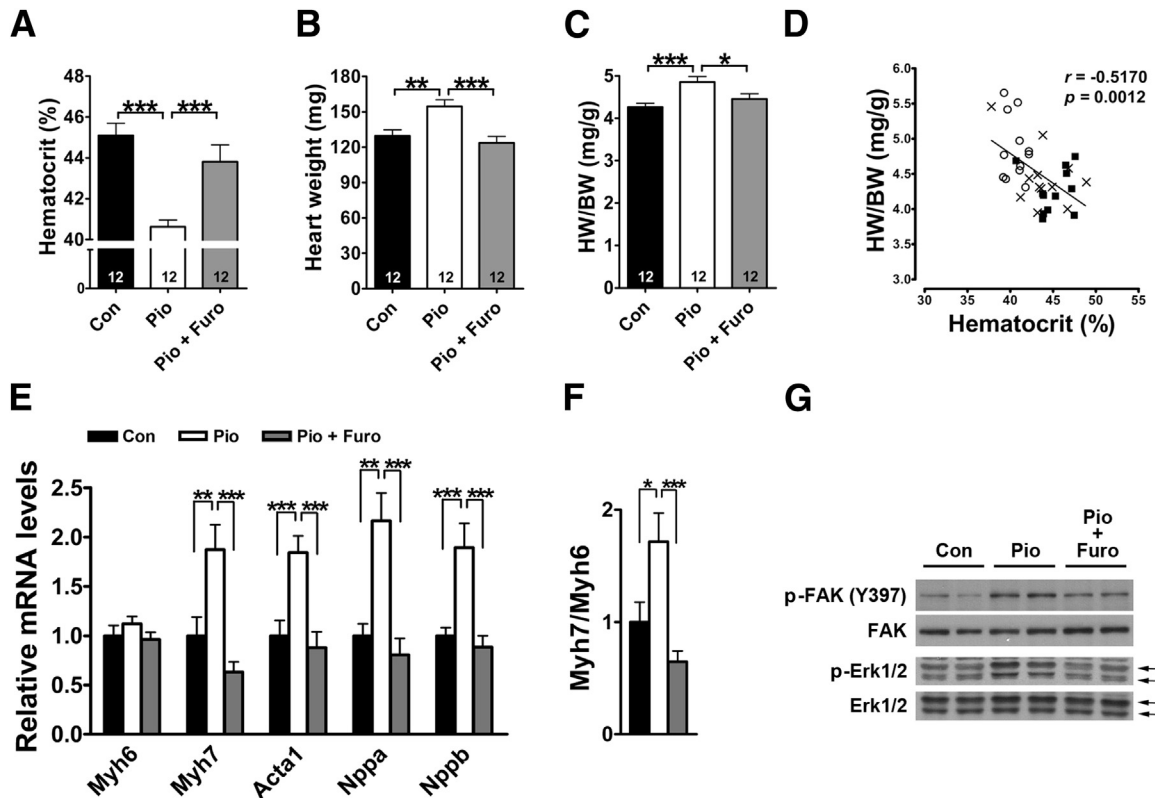


Figure 4 Effects of furosemide on pioglitazone-induced volume expansion and CH. **A–C:** Hematocrit (**A**), HW (**B**), and HW/BW ratio (**C**) of control, pioglitazone-treated, and pioglitazone+furosemide-treated mice. **D:** Correlation between HW/BW ratio and hematocrit in control (squares), pioglitazone-treated (circles), and pioglitazone+furosemide-treated mice (crosses). $n = 12$ mice per group. **E** and **F:** Expression of contractile and natriuretic peptide genes (**E**) and the Myh7/Myh6 ratio (**F**). mRNA levels are expressed relative to average expression in control mice. **G:** Immunoblot analyses of phosphorylation of FAK and Erk1/2 in the heart. Bands and arrows are as described for Figure 3. Data are expressed as means \pm SEM. $n = 12$ mice per group. * $P < 0.05$, ** $P < 0.01$, and *** $P < 0.001$, Fisher's LSD test. Pio, pioglitazone.

glycogenolysis were not affected by rosiglitazone or rosiglitazone+furosemide (Supplemental Figure S6). However, mRNA levels of Pdk4, which inhibits glucose utilization by reducing conversion of pyruvate into acetyl-CoA, were dramatically down-regulated by rosiglitazone (Figure 6A). Importantly, normalization of CH by cotreatment with furosemide did not inhibit rosiglitazone-induced Pdk4 down-regulation.

Among the molecules involved in cellular fatty acid transport, mRNA levels of lipoprotein lipase (*Lpl*) were not affected by rosiglitazone or rosiglitazone+furosemide (Supplemental Figure S6). Although fatty acid translocase (*Cd36*) was up-regulated, fatty acid transporter member 1 (FATP1; *Slc27a1*) was down-regulated in both groups (Figure 6B). Surprisingly, genes involved in mitochondrial fatty acid oxidation [carnitine palmitoyltransferase 1b and 2 (*Cpt1b* and *Cpt2*); acyl-coenzyme A dehydrogenase, long chain (*Acadl*); *Acadm*; and mitochondrial uncoupling protein 3 (*Ucp3*)] were significantly down-regulated by rosiglitazone treatment (Figure 6C). Cotreatment with furosemide did not attenuate rosiglitazone-induced down-regulation of these genes. Moreover, the down-regulation of fatty acid oxidation appears to be specific to mitochondria, because mRNA levels of peroxisomal acyl-coenzyme A

oxidase 1 (*Acox1*) was not affected by either rosiglitazone or rosiglitazone+furosemide (Supplemental Figure S6). These findings suggest that rosiglitazone-induced CH is associated with down-regulation of mitochondrial fatty acid oxidation, but that amelioration of plasma overload and CH does not affect the down-regulated mitochondrial fatty acid oxidation. These findings further suggest that rosiglitazone treatment shifts metabolism genes toward glucose-usage preference, independent of volume expansion. Similarly, pioglitazone treatment also shifted metabolism genes toward glucose-usage preference, and cotreatment with furosemide did not attenuate these changes (Supplemental Figure S7). Consistent with the metabolism gene expression pattern, rosiglitazone treatment significantly decreased heart triglyceride content, and furosemide cotreatment did not attenuate this change (Figure 6D).

Furosemide Cotreatment Does Not Compromise Whole-Body Insulin-Sensitizing Effects of TZD

Finally, we investigated whether furosemide cotreatment affects the insulin-sensitizing activity of rosiglitazone. Mice fed the control high-fat diet for 4 weeks exhibited compromised

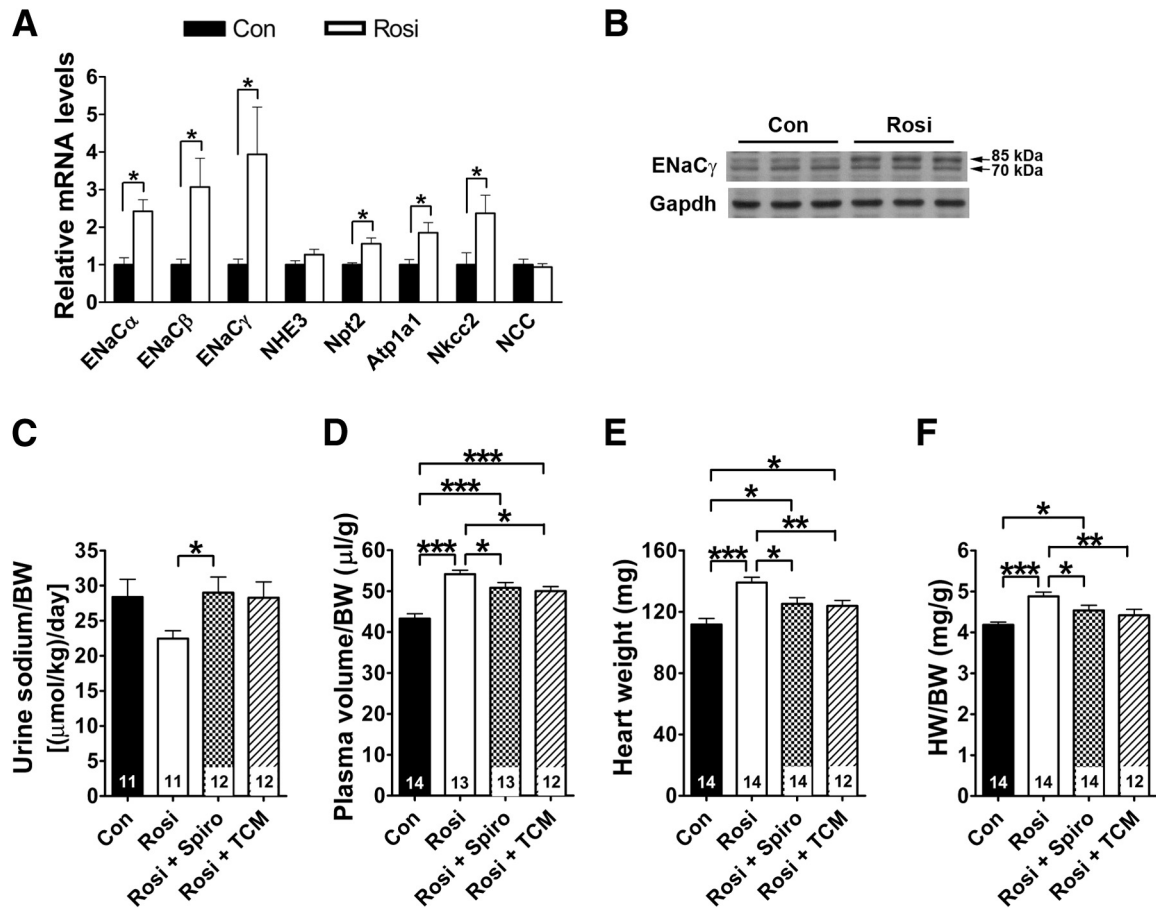


Figure 5 Effects of spironolactone and TCM on rosiglitazone-induced volume expansion and CH. **A:** Expression of sodium transporter genes in renal tubule in the kidneys of control and rosiglitazone-treated mice. mRNA levels are expressed relative to average expression in control mice. **B:** Immunoblot analyses of ENaC γ in the kidney. Each band represents a single mouse; both 85- and 70-kDa bands represent ENaC γ . **C–F:** Daily sodium excretion (**C**), plasma volume (**D**), HW (**E**), and HW/BW ratio (**F**) of control, rosiglitazone-treated, rosiglitazone+spironolactone-treated, and rosiglitazone+TCM-treated mice. Data are expressed as means \pm SEM. $n = 6$ (**A**) or 11–14 (**C–F**) mice per group (indicated on data bars). * $P < 0.05$, ** $P < 0.01$, and *** $P < 0.001$, Student's t -test (**A**) or Fisher's LSD test (**C–F**). Spiro, spironolactone.

metabolic parameters (Table 2). Supplementing this high-fat diet with rosiglitazone effectively attenuated many of the metabolic parameters, although total BW and gonadal fat mass were not altered. In contrast, rosiglitazone treatment caused a significant increase in inguinal fat mass, suggesting that a greater portion of lipids are channeled to subcutaneous adipose tissue by PPAR γ activation. This resulted in reduction of the intraperitoneal/subcutaneous fat mass ratio; a lower ratio is generally considered to reflect a preferable distribution of body fat. Rosiglitazone treatment attenuated impairments of glucose metabolism, as evidenced by lower levels of plasma insulin, fatty acids, and glucose, as well as lower homeostatic model assessment (HOMA) index and higher plasma adiponectin levels, relative to control treatment.

Importantly, metabolic parameters in mice cotreated with rosiglitazone and furosemide did not differ from those in mice treated with rosiglitazone alone, except that mice in the cotreatment group consumed more water, indicative of thirst resulting from diuresis. These findings demonstrate that release of volume overload does not compromise either the

insulin-sensitizing effects of TZD or the improvement of glucose homeostasis.

Discussion

With the present study, we have demonstrated that rosiglitazone-induced CH in mice is mediated through PPAR γ activation and requires intact ligand-binding ability of PPAR γ . We further demonstrated that releasing volume overload attenuates rosiglitazone-induced CH, hypertrophic gene reprogramming, cardiomyocyte apoptosis, hypertrophy-related signal activation, and LV dysfunction. These effects are therefore attributable to volume expansion and are unlikely to be direct effects of rosiglitazone in the heart. In contrast, expression of glucose and lipid metabolism genes in the heart was altered by rosiglitazone, but these changes were not attenuated by release of volume overload, suggesting that regulation of nutrient metabolism genes is independent of volume expansion but dependent on presence of rosiglitazone.

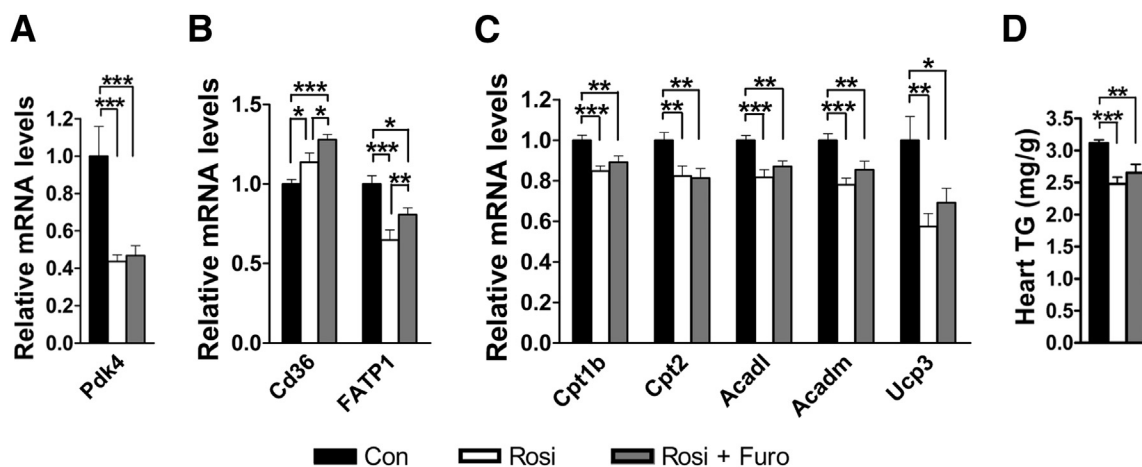


Figure 6 Expression of glucose and lipid metabolism genes in rosiglitazone-induced CH. Expression of genes for glucose utilization (A), lipid transport (B), and fatty acid oxidation (C) and triglyceride contents (D) in the hearts of control, rosiglitazone-treated, and rosiglitazone+furosemide-treated mice. mRNA levels are expressed relative to average expression in control mice. Data are expressed as means \pm SEM. $n = 12$ mice per group. * $P < 0.05$, ** $P < 0.01$, and *** $P < 0.001$, Fisher's LSD test. TG, triglyceride.

One approach to addressing PPAR γ dependence of TZD-induced CH would be the use of PPAR γ -deficient mice. In the present study, rosiglitazone-induced volume expansion and CH were attenuated in *Pparg*^{P465L/+} mice, but not in *Pparg*^{+/-} mice. Although the genetic backgrounds of the *Pparg*^{P465L/+} and *Pparg*^{+/-} mice described here are different, the effect of rosiglitazone on CH was also blunted in *Pparg*^{P465L/+} mice on a 129S6:C57BL/6 F1 background (data not shown). This indicates that 50% normal expression of PPAR γ is sufficient to mediate rosiglitazone-induced CH, but that the dominant-negative effect of ligand-binding defective PPAR γ attenuates rosiglitazone-induced CH.

It has been suggested that both cardiac and noncardiac PPAR γ activity contribute to TZD-induced CH. In a study by Duan et al,²¹ rosiglitazone treatment of cardiac-specific PPAR γ knockout mice with 10 mg/kg per day for 4 weeks caused CH, but to a lesser extent than in rosiglitazone-treated WT mice. In terms of the role of PPAR γ in noncardiac tissues, two studies demonstrated that renal PPAR γ activation by TZDs up-regulates ENaC γ and increases water reabsorption.^{9,10} Although TZD-induced hemodilution occurred only in the presence of intact collecting-duct PPAR γ , those studies did not address effects of collecting-duct PPAR γ on TZD-induced CH. In the present study, the

Table 2 Metabolic and Physiological Measurements

Measure	Regular chow	High-fat diet		
		Control	Rosiglitazone	Rosiglitazone + furosemide
BW (g)	27.6 \pm 0.8	30.3 \pm 0.7	31.2 \pm 0.6	29.9 \pm 0.5
Gonadal weight/BW (mg/g)	10.4 \pm 1.0	23.8 \pm 2.1	23.3 \pm 1.1	21.3 \pm 1.6
HW/Body length (mg/cm)	13.3 \pm 0.5	13.5 \pm 0.3	15.6 \pm 0.4***	13.6 \pm 0.3 [†]
Inguinal weight/BW (mg/g)	6.9 \pm 0.5	11.9 \pm 0.7	18.2 \pm 0.9***	15.7 \pm 1.1**
Gonadal weight/inguinal weight (mg/mg)	1.51 \pm 0.09	1.95 \pm 0.07	1.29 \pm 0.03***	1.35 \pm 0.03***
Insulin (ng/mL)	0.14 \pm 0.05	3.12 \pm 0.71	0.74 \pm 0.16**	1.14 \pm 0.44*
Glucose (mg/dL)	134 \pm 14	257 \pm 20	201 \pm 9*	173 \pm 13***
HOMA index	1.2 \pm 0.5	52.3 \pm 16.0	9.3 \pm 2.4**	13.5 \pm 6.6*
Free fatty acid (mEq/L)	0.40 \pm 0.04	0.77 \pm 0.11	0.35 \pm 0.03***	0.42 \pm 0.03**
Adiponectin (μ g/mL)	ND	5.2 \pm 0.4	13.0 \pm 0.4***	12.2 \pm 0.7***
Mean blood pressure (mmHg)	ND	98 \pm 1	89 \pm 2**	92 \pm 1*
Water consumption (mL/day per mouse)	ND	4.8 \pm 0.4	4.2 \pm 0.2	11 \pm 0.4*** [†]
Food consumption (g/day per mouse)	ND	2.36 \pm 0.13	2.49 \pm 0.15	2.50 \pm 0.07

The data for the regular chow group ($n = 3$ to 12) were obtained in separate experiments from those for the experimental high-fat diet groups and were not included in the statistical analyses. For high-fat diet experiments, $n = 5$ mice per group for free fatty acid and blood pressure; $n = 6$ for insulin, glucose, HOMA index, and adiponectin; $n = 10$ or 11 for food consumption; and $n = 27$ for all other measurements.

* $P < 0.05$, ** $P < 0.01$, and *** $P < 0.001$ versus control, Fisher's LSD test.

[†] $P < 0.001$ versus rosiglitazone, Fisher's LSD test.

ND, not determined.

extent of CH was strongly correlated with the extent of volume expansion. Furthermore, effective reduction of hypertrophy by release of plasma volume with diuretics confirms the dependence of TZD-induced CH on volume expansion due to PPAR γ activation in noncardiac tissues. Diuretic agents typically decrease blood pressure in addition to reducing blood volume, which may contribute to reduced CH and dysfunction. Rosiglitazone decreased mean blood pressure, and that furosemide cotreatment did not cause further changes in blood pressure (Table 2). These findings suggest that the inhibition of CH by furosemide cotreatment is not likely attributable to change in blood pressure.

Mechanical stretch triggers FAK phosphorylation, followed by recruitment of Erk1/2 to FAK and activation of Erk1/2 during increased myocardial workload.¹⁸ Erk1/2 activation regulates expression of structural and hypertrophy-responsive genes through phosphorylation and activation of transcription factors, such as Gata4 and Elk1.²² Our findings suggest that volume expansion by TZD treatment increases mechanical stretch and so triggers FAK and Erk1/2 activation. Impeding volume expansion prevents FAK and Erk1/2 activation, and so prevents subsequent dysregulation of hypertrophy-responsive genes. Thus, FAK and Erk1/2 activation is critical in TZD-induced volume overload and CH.

How does volume expansion lead to cardiac dysfunction during rosiglitazone treatment? Volume overload increases stretching force on the myocardium and leads to myocardial apoptosis. Apoptosis of cardiomyocytes then reduces the contractile force, contributing to progressive LV dysfunction.^{23,24} In the present study, rosiglitazone-induced volume expansion was associated with increased myocardial apoptosis and LV dysfunction. Release of volume expansion ameliorated both apoptosis and LV dysfunction, implicating a volume expansion–apoptosis–LV dysfunction axis in rosiglitazone-induced CH.

Although our findings of a significant increase in expression of three subunits of ENaC are compatible with the notion that rosiglitazone-induced fluid retention is mediated by activation of ENaC, recent studies argue against ENaC in TZD-mediated fluid retention. For example, several research groups found no change or even decreases in expression of ENaC subunit in rodents or in cultured cells treated with TZDs.^{25,26} Functional inactivation of ENaC α did not protect animals against rosiglitazone-induced fluid retention.²⁷ Furthermore, and in contrast, chronic rosiglitazone treatment improved renal handling of salt and water in rats with pre-existing heart failure.²⁸ Efficacy of amiloride in alleviating PPAR γ agonist-induced fluid retention also remains debatable.²⁹ In the present study, cotreatment with amiloride did not prevent rosiglitazone-induced volume expansion and CH. Treatment with a higher dose of amiloride (0.1 mg/mL in drinking water) affected appetite and caused BW loss (data not shown). These findings argue against stimulation of ENaC as the initial target of PPAR γ agonist-mediated fluid retention and suggest involvement of renal transporters other than ENaC in rosiglitazone-induced water reabsorption.

Short-term (3-day) treatment with rosiglitazone increases protein levels of Atp1a1, Npt2, and NHE3 in the proximal convoluted tubule and of Nkcc2 in the thick ascending limb.⁸ In accord, our results with a relatively long-term rosiglitazone treatment (4 weeks) also demonstrated upregulation of mRNA levels of Atp1a1, Npt2, and Nkcc2. Although mRNA or protein abundance does not always reflect membrane-bound transporter activity, further attention should be focused on ENaC γ and other sodium transporters of renal tubule in rosiglitazone-induced sodium reabsorption. One clinical trial with an acute diuretic treatment (7 days) showed that rosiglitazone-induced hemodilution was reversed by treatment with spironolactone or thiazides (hydrochlorothiazide), but not with furosemide.¹² Another clinical trial, however, showed preserved response to furosemide in rosiglitazone-treated insulin-resistant subjects.¹³ In our rodent model with 4-week diuretic treatment, furosemide attenuated rosiglitazone-induced volume expansion and CH to an extent similar to that observed with spironolactone or TCM. Spironolactone is known to block aldosterone receptor–mediated sodium reabsorption. Thus, in addition to ENaC, other transporters (including NHE3, NCC, and Atp1a1) are affected by spironolactone.³⁰ This may explain why spironolactone is more effective than amiloride in release of rosiglitazone-mediated dysregulation in sodium balance and volume handling. On the other hand, although our findings did not suggest a role of NCC in rosiglitazone-induced fluid retention (as indicated by unchanged NCC expression in rosiglitazone treatment), forced inhibition of NCC by TCM effectively protected mice against rosiglitazone-induced volume expansion and CH. Thus, therapy against TZD-induced volume expansion is not necessarily limited to targeting the specific transporters whose expression is affected during TZD treatment.

The mechanism of TZDs in increasing insulin sensitivity is redirection of lipid to adipose tissues, which is orchestrated by adipose PPAR γ in coordination with nonadipose PPAR γ . Thus, the *in vivo* effects of TZDs on the heart are complicated by changes in plasma and tissue lipid metabolism. The present study, together with those of others,^{7,31} clearly demonstrates a paradoxical reduction in cardiac expression of many PPAR γ downstream genes, including those for lipid transport and fatty acid oxidation. Similarly, we also found that rosiglitazone treatment led to a change in nutrient-usage preference from fatty acids to carbohydrates in the heart. This is coordinated by down-regulation of genes for glycolysis inhibition (*Pdk4*) and mitochondrial fatty acid oxidation in the heart. Redirection of lipid to adipose tissue is also evidenced by reduction of heart triglyceride content and increase in subcutaneous inguinal fat weight. Importantly, the shift of energy preference to glucose in the heart and the redirection of lipid to adipose tissue are not inhibited by release of volume overload, despite reversal of increase in heart mass, suggesting that these actions of TZDs are not likely to be the major cause of

CH. In addition, the effect of furosemide is relatively brief; in the present study, volume expansion and CH reappeared after discontinuing furosemide administration for 1 week. Thus, coprescription of diuretics and hematocrit monitoring are advised for patients being treated with TZDs.

In our study, furosemide cotreatment did not affect insulin-sensitizing activity of rosiglitazone, even though some values in the cotreatment group showed a slight attenuation (Table 2). It is likely that the parameters in blood are affected by plasma volume, because furosemide has been reported to increase lipid levels by changing the intravascular volume.³² In summary, our results provide direct evidence that cotreatment with diuretics can reduce adverse effects of TZD-induced volume expansion and cardiac events without compromising the action of TZD on glucose usage in the heart and without compromising whole-body insulin sensitivity. This cotreatment strategy could be adopted immediately, without withdrawal of TZDs and testing new drugs that target PPAR γ .

Acknowledgments

We thank Dr. Ronald Evans for the *Pparg*^{+/-} mice, Dr. Sheng-Hsiang Lin for suggestions on statistical analysis, and Ya-Yun Shih for technical assistance of echocardiography.

Supplemental Data

Supplemental material for this article can be found at <http://dx.doi.org/10.1016/j.ajpath.2013.10.020>.

References

- Nissen SE, Wolski K: Effect of rosiglitazone on the risk of myocardial infarction and death from cardiovascular causes [Erratum appeared in *N Engl J Med* 2007, 357:100]. *N Engl J Med* 2007, 356:2457–2471
- Lago RM, Singh PP, Nesto RW: Congestive heart failure and cardiovascular death in patients with prediabetes and type 2 diabetes given thiazolidinediones: a meta-analysis of randomised clinical trials. *Lancet* 2007, 370:1129–1136
- Rosen CJ: The rosiglitazone story—lessons from an FDA Advisory Committee meeting. *N Engl J Med* 2007, 357:844–846
- Rangwala SM, Lazar MA: Peroxisome proliferator-activated receptor gamma in diabetes and metabolism. *Trends Pharmacol Sci* 2004, 25:331–336
- Lehman JJ, Kelly DP: Gene regulatory mechanisms governing energy metabolism during cardiac hypertrophic growth. *Heart Fail Rev* 2002, 7:175–185
- Kurtz DM, Rinaldo P, Rhead WJ, Tian L, Millington DS, Vockley J, Hamm DA, Brix AE, Lindsey JR, Pinkert CA, O'Brien WE, Wood PA: Targeted disruption of mouse long-chain acyl-CoA dehydrogenase gene reveals crucial roles for fatty acid oxidation. *Proc Natl Acad Sci USA* 1998, 95:15592–15597
- Son NH, Park TS, Yamashita H, Yokoyama M, Huggins LA, Okajima K, Homma S, Szabolcs MJ, Huang LS, Goldberg IJ: Cardiomyocyte expression of PPARgamma leads to cardiac dysfunction in mice. *J Clin Invest* 2007, 117:2791–2801
- Song J, Knepper MA, Hu X, Verbalis JG, Ecelbarger CA: Rosiglitazone activates renal sodium- and water-reabsorptive pathways and lowers blood pressure in normal rats. *J Pharmacol Exp Ther* 2004, 308:426–433
- Guan Y, Hao C, Cha DR, Rao R, Lu W, Kohan DE, Magnuson MA, Redha R, Zhang Y, Breyer MD: Thiazolidinediones expand body fluid volume through PPARgamma stimulation of ENaC-mediated renal salt absorption. *Nat Med* 2005, 11:861–866
- Zhang H, Zhang A, Kohan DE, Nelson RD, Gonzalez FJ, Yang T: Collecting duct-specific deletion of peroxisome proliferator-activated receptor gamma blocks thiazolidinedione-induced fluid retention. *Proc Natl Acad Sci USA* 2005, 102:9406–9411
- Katz AM: Cardiomyopathy of overload. A major determinant of prognosis in congestive heart failure. *N Engl J Med* 1990, 322:100–110
- Karalliedde J, Buckingham R, Starkie M, Lorand D, Stewart M, Viberti G; Rosiglitazone Fluid Retention Study Group: Effect of various diuretic treatments on rosiglitazone-induced fluid retention. *J Am Soc Nephrol* 2006, 17:3482–3490
- Rennings AJ, Russel FG, Li Y, Deen PM, Masereeuw R, Tack CJ, Smits P: Preserved response to diuretics in rosiglitazone-treated subjects with insulin resistance: a randomized double-blind placebo-controlled crossover study. *Clin Pharmacol Ther* 2011, 89:587–594
- Tsai YS, Kim HJ, Takahashi N, Kim HS, Hagaman JR, Kim JK, Maeda N: Hypertension and abnormal fat distribution but not insulin resistance in mice with P465L PPARgamma. *J Clin Invest* 2004, 114:240–249
- Kis A, Murdoch C, Zhang M, Siva A, Rodriguez-Cuenca S, Carobbio S, Lukasik A, Blount M, O'Rahilly S, Gray SL, Shah AM, Vidal-Puig A: Defective peroxisomal proliferators activated receptor gamma activity due to dominant-negative mutation synergizes with hypertension to accelerate cardiac fibrosis in mice. *Eur J Heart Fail* 2009, 11:533–541
- Asakawa M, Takano H, Nagai T, Uozumi H, Hasegawa H, Kubota N, Saito T, Masuda Y, Kadowaki T, Komuro I: Peroxisome proliferator-activated receptor gamma plays a critical role in inhibition of cardiac hypertrophy in vitro and in vivo. *Circulation* 2002, 105:1240–1246
- Sugden PH, Clerk A: "Stress-responsive" mitogen-activated protein kinases (c-Jun N-terminal kinases and p38 mitogen-activated protein kinases) in the myocardium. *Circ Res* 1998, 83:345–352
- Domingos PP, Fonseca PM, Nadruz W Jr., Franchini KG: Load-induced focal adhesion kinase activation in the myocardium: role of stretch and contractile activity. *Am J Physiol Heart Circ Physiol* 2002, 282:H556–H564
- Juurlink DN, Gomes T, Lipscombe LL, Austin PC, Hux JE, Mamdani MM: Adverse cardiovascular events during treatment with pioglitazone and rosiglitazone: population based cohort study. *BMJ* 2009, 339:b2942
- Caglayan E, Stauber B, Collins AR, Lyon CJ, Yin F, Liu J, Rosenkranz S, Erdmann E, Peterson LE, Ross RS, Tangirala RK, Hsueh WA: Differential roles of cardiomyocyte and macrophage peroxisome proliferator-activated receptor gamma in cardiac fibrosis. *Diabetes* 2008, 57:2470–2479
- Duan SZ, Ivashchenko CY, Russell MW, Milstone DS, Mortensen RM: Cardiomyocyte-specific knockout and agonist of peroxisome proliferator-activated receptor-gamma both induce cardiac hypertrophy in mice. *Circ Res* 2005, 97:372–379
- Bueno OF, Molkentin JD: Involvement of extracellular signal-regulated kinases 1/2 in cardiac hypertrophy and cell death. *Circ Res* 2002, 91:776–781
- Mihl C, Dassen WR, Kuipers H: Cardiac remodelling: concentric versus eccentric hypertrophy in strength and endurance athletes. *Neth Heart J* 2008, 16:129–133
- Khoyezhad A, Jalali Z, Tortolani AJ: Apoptosis: pathophysiology and therapeutic implications for the cardiac surgeon. *Ann Thorac Surg* 2004, 78:1109–1118
- Borsting E, Cheng VP, Glass CK, Vallon V, Cunard R: Peroxisome proliferator-activated receptor-gamma agonists repress epithelial

- sodium channel expression in the kidney. *Am J Physiol Renal Physiol* 2012, 302:F540–F551
26. Nofziger C, Blazer-Yost BL: PPARgamma agonists, modulation of ion transporters, and fluid retention. *J Am Soc Nephrol* 2009, 20:2481–2483
 27. Vallon V, Hummler E, Rieg T, Pochynyuk O, Bugaj V, Schroth J, Dechenes G, Rossier B, Cunard R, Stockand J: Thiazolidinedione-induced fluid retention is independent of collecting duct alphaENaC activity. *J Am Soc Nephrol* 2009, 20:721–729
 28. Goltzman I, Wang X, Lavallie ER, Diblasio-Smith EA, Ovcharenko E, Hoffman A, Abassi Z, Feuerstein GZ, Winaver J: Effects of chronic rosiglitazone treatment on renal handling of salt and water in rats with volume-overload congestive heart failure. *Circ Heart Fail* 2011, 4: 345–354
 29. Chen L, Yang B, McNulty JA, Clifton LG, Binz JG, Grimes AM, Strum JC, Harrington WW, Chen Z, Balon TW, Stimpson SA, Brown KK: G1262570, a peroxisome proliferator-activated receptor {gamma} agonist, changes electrolytes and water reabsorption from the distal nephron in rats. *J Pharmacol Exp Ther* 2005, 312:718–725
 30. Booth RE, Johnson JP, Stockand JD: Aldosterone. *Adv Physiol Educ* 2002, 26:8–20
 31. Festuccia WT, Laplante M, Brûlé S, Houde VP, Achouba A, Lachance D, Pedrosa ML, Silva ME, Guerra-Sá R, Couet J, Arsenault M, Marette A, Deshaies Y: Rosiglitazone-induced heart remodelling is associated with enhanced turnover of myofibrillar protein and mTOR activation. *J Mol Cell Cardiol* 2009, 47: 85–95
 32. Campbell N, Brant R, Stalts H, Stone J, Mahallati H: Fluctuations in blood lipid levels during furosemide therapy: a randomized, double-blind, placebo-controlled crossover study. *Arch Intern Med* 1998, 158:1461–1463